Elsevier required licence: © <2021>. This manuscript version is made available under the CC-BY-NC-ND 4.0 license http://creativecommons.org/licenses/by-nc-nd/4.0/
The definitive publisher version is available online at
[https://www.sciencedirect.com/science/article/pii/S0269749120365015?via%3Dihub]

Oil spill trajectory modelling and environmental vulnerability mapping using GNOME model and GIS

Abdul-Lateef Balogun[1], Shamsudeen Temitope Yekeen[2*], Biswajeet Pradhan[3,4,5,6] and Khamaruzaman B. Wan Yusof [7]

[1,2]Geospatial Analysis and Modelling (GAM) Research Group, Department of Civil and Environmental Engineering, Universiti Teknologi PETRONAS (UTP), 32610 Seri Iskandar, Perak, Malaysia.

[3]Center for Advanced Modeling and Geospatial Information Systems (CAMGIS), Faculty of Engineering and IT, University of Technology Sydney, Sydney, NSW 2007, Australia

[4]Department of Energy and Mineral Resources Engineering, Sejong University, Choongmu-gwan, 209 Neungdong-ro, Gwangjin-gu, Seoul 05006, Korea

[5]Center of Excellence for Climate Change Research, King Abdulaziz University, P. O. Box 80234, Jeddah 21589, Saudi Arabia

[6]Earth Observation Center, Institute of Climate Change, Universiti Kebangsaan Malaysia, 43600 UKM, Bangi, Selangor, Malaysia

[7]Department of Civil and Environmental Engineering, Universiti Teknologi PETRONAS (UTP), 32610 Seri Iskandar, Perak, Malaysia.

* Corresponding Author: Shamsudeenyekeen1@gmail.com;Temishams@gmail.com

Abstract

This study develops an oil spill environmental vulnerability model for predicting and mapping the oil slick trajectory pattern in Kota Tinggi, Malaysia. The impact of seasonal variations on the vulnerability of the coastal resources to oil spill was modelled by estimating the quantity of coastal resources affected across three climatic seasons (northeast monsoon, southwest monsoon and pre-monsoon). Twelve 100m^3 (10,000 splots) medium oil spill scenarios were simulated using General National Oceanic and Atmospheric Administration Operational Oil Modeling Environment (GNOME) model. The output was integrated with coastal resources, comprising biological, socio-economic and physical shoreline features. Results revealed that the speed of an oil slick (40.8 meters per minute) is higher during the pre-monsoon period in a southwestern direction and lower during the northeast monsoon (36.9 meters per minute). Evaporation, floating and spreading are the major weathering processes identified in this study, with approximately 70% of the slick reaching the shoreline or remaining in the water column during the first 24 hours (h) of the spill. Oil spill impacts were most severe during the southwest monsoon, and physical shoreline resources are the most vulnerable to oil spill in the study area. The study concluded that variation in climatic seasons significantly influence the vulnerability of coastal resources to marine oil spill.

Keywords: Oil spill; trajectory modelling; vulnerability mapping; GNOME model; GIS; Malaysia

1.0 Introduction

The importance of crude oil as a major contributor to global development and it has been documented in several literature (Guo, 2017, Van Winden et al., 2013, Jiang et al., 2012, Kilian, 2010, Hamilton and Wu, 2014). This is for its contributions to government revenue, creating employment opportunities and energy supply (Guo, 2017). The tremendous increase in world population over the years (Yekeen et al., 2019) has escalated the oil production rate to about 9947 billion ton-miles (Chen et al., 2019) and a high percentage of it is transported by sea yearly (Alaa El-Din et al., 2018). This results in oil spill at different scales and frequency (Balogun et al., 2018). Oil spills usually occur through ship collision, wrecking, pipeline blowing, refinery activities, pipeline vandalism, sabotage, and ship tank cleaning (Lee et al., 2015, Clark, 1992, Blackburn et al., 2014, Li et al., 2016).

Oil spills pose severe threats to coastal ecosystems, ranging from immediate economic losses to long-term adverse effects on the interactions between ecological elements (Yang et al., 2011). This is because of its densely populated configuration (Statham, 2012, Halpern et al., 2015). Similarly, the locational interface (Menicagli et al., 2019) of coastal ecosystem makes it highly vulnerable to anthropogenic pollutants (Ferreira et al., 2017) such as plastic debris (Zhang, 2017, Menicagli et al., 2019, Yekeen et al., 2019), metal debris, volatile methylsiloxanes (Rocha et al., 2019) and oil spills. On a global estimate between 1970-2015, over 238 marine oil spill incidents have occurred close to coastal environments, affecting large expanse of vegetation, sand beach, marine mammals, and birds (Sheppard, 2000, Beyer et al., 2016, Piatt et al., 1990, Trustees, 2016, Mignucci-Giannoni, 1999).

In many parts of the world, a large percentage of oil spill effects on coastal ecosystems is linked to the unavailability of reliable Decision Support Systems (DSS) which can accurately delineate the vulnerable coastal resources for prompt intervention (Melaku Canu et al., 2015, Kankara et al., 2016, Balogun et al., 2018, Temitope Yekeen et al., 2020). DSSs help to reduce the consequence of oil spills on the coastal environment by forecasting vulnerable areas and resources to aid rapid response.

Vulnerability is a nebulous word which requires contextual definition. Broadly, vulnerability assessment entails identifying areas with potential to suffer loss, damage, or injury as a result of an action. It involves the mapping and presentation of probable information on the areas that are likely to be affected by the occurrence of hazards like marine oil spill (Romero et al., 2013). In the past, a good deal of oil spill vulnerability assessments have been done based on worst case, average and survey based approaches. Castanedo et al. (2009) considered socio-economic, physical and biological features of Cantabria coast to classify the area's vulnerability to oil spill impacts into high, moderate and low vulnerability levels. Depellegrin and Pereira (2016) adopted similar procedures to classify vulnerable locations within 237 km of the shoreline using physical and biological properties of the area, with consideration of shoreline sinuosity, orientation and wave exposure. Azevedo et al. (2017) developed a web-based GIS (geographical information systems) for the prediction of oil spill vulnerability based on the physical, socio-economic, biological and global vulnerability index of the intertidal area of the water body. However, a major shortcoming of these approaches is the absence of definite vulnerability level of the coastal environment to different types of spill scenarios (e.g. pipeline leakage) and spill intensity, as well as the possibility of uncertainty and subjectivity in experts' opinions.

To overcome the limitations of expert systems, different mathematical models have been developed to date (Guo et al., 2014, Qiao et al., 2019, Nordam et al., 2019, Bozkurtoğlu, 2017, Liu et al., 2015). These include Oil Spill Contingency and Response (OSCAR), General National Oceanic and Atmospheric Administration Operational Oil Modeling Environment (GNOME), Medslik-II, Spill Impact Model Application Package (SIMAP), Oil Modeling Application Package (OILMAP), the operational system METEO-MOHID for the Prestigue-Nassua oil spill, and OILTRANS for the Northwest European continental shelf (Gług and Wąs, 2018, Chiu et al., 2018, Liu et al., 2015, Nordam et al., 2019, Qiao et al., 2019). More recently, the semi-implicit cross-scale hydro-science integrated system model (SCHISM) which uses water surface elevation and currents for oil spill trajectory has been developed (Chiu et al., 2018). These models have been applied in different studies globally (Depellegrin and Pereira, 2016, Kankara et al., 2016, Azevedo et al., 2017, Bozkurtoğlu, 2017, Balogun et al., 2018, Chiu et al., 2018, Gług and Wąs, 2018, Amir-Heidari and Raie, 2019, Nordam et al., 2019, Qiao et al., 2019, Biswajeet et al., 2009), with the limitation of not taking into consideration climatic variations which cause changes in environmental parameters that influence oil spill trajectory prediction and emergency response planning. Satpathy et al. (2010), Akhir et al. (2011), Abdul-Hadi et al. (2013) indicated that variation in the salinity, temperature, freshwater discharge and speed of ocean conditions contribute to the flow and movement of objects (e.g. oil spill) on ocean surface. Although some countries (e.g. U.K) require that trajectory modelling needs to incorporate meteorological parameters (Department for Business, 2019) such climatic scenario testing and analysis is not common in literature.

Therefore, a novel coastal decision support system that considers climatic conditions for rapid identification of vulnerable areas and resources is essential. Vulnerability in this context is the likelihood of an oil spill reaching and affecting specific features of interest within the study area. Thus, this study addresses this gap by pursuing the following objectives: i) model and predict oil slick trajectory in the study area; ii) estimate the impact of climatic variations on coastal resources during oil spill; and iii) assess the vulnerability level of the different coastal resources to the oil spill.

The other sections of the study are organized as follows: Section 2 gives a broad background on the study area and the rationale for the choice of location. Section 3 states the materials used, including the sources of data and the methods adopted. This comprises the trajectory model and the spatial analysis performed to produce seasonal environmental sensitivity maps. Section 4 gives a critical analysis of the results and discusses the major findings, and Section 5 presents the conclusion of the study.

2.0 Study Area

Peninsular Malaysia contains eleven states, including Johor. The state of Johor is located between 1^{0}13’30”N-1^{0}54’30”N and 103^{0}35’00”E-104^{0}16’0”E, covering approximately 19,102 km^2 land area (Malaysia, 2013) and has four districts: Kota Tinggi, Kluang, Kulai Jaya and Johor Bahru (Tan et al., 2015) with eight major towns. Johor is bounded by straits of Malacca to the west, straits of Johor to the south and China Sea to the east. It has a total of 400 km of coastline, majorly at the east and west which are predominantly habitats of mangrove, swampy wetland, grasses and Niplah forest (Abdul Karim et al., 2004). High percentage of oil palm production is carried out in Johor because of its fertile land (Tan et al., 2015) and it is renowned for its intensive port activities, comprising of domestic and international marine transportation. The coastal city is highly vulnerable to oil spills, especially Kota Tinngi (Sakari et al., 2010) because of the frequent use and movement of petroleum products that are often discharged into the water body. Similarly, its proximity to the China sea, which experiences intense cargo vessel movements, exacerbates its vulnerability to oil spill pollution (Nagarajan et al., 2013). For this study, the coastal area of Kota Tinggi with approximately 196 km shoreline (See Figure 1) between 2^{0}39’53.07”N-1^{0}21’36.02”N and 103^{0} 38’14.82”E-104^{0}16’5.74”E was used due to the frequent occurrence of oil spill in this region caused by the recurrent transportation of crude oil.

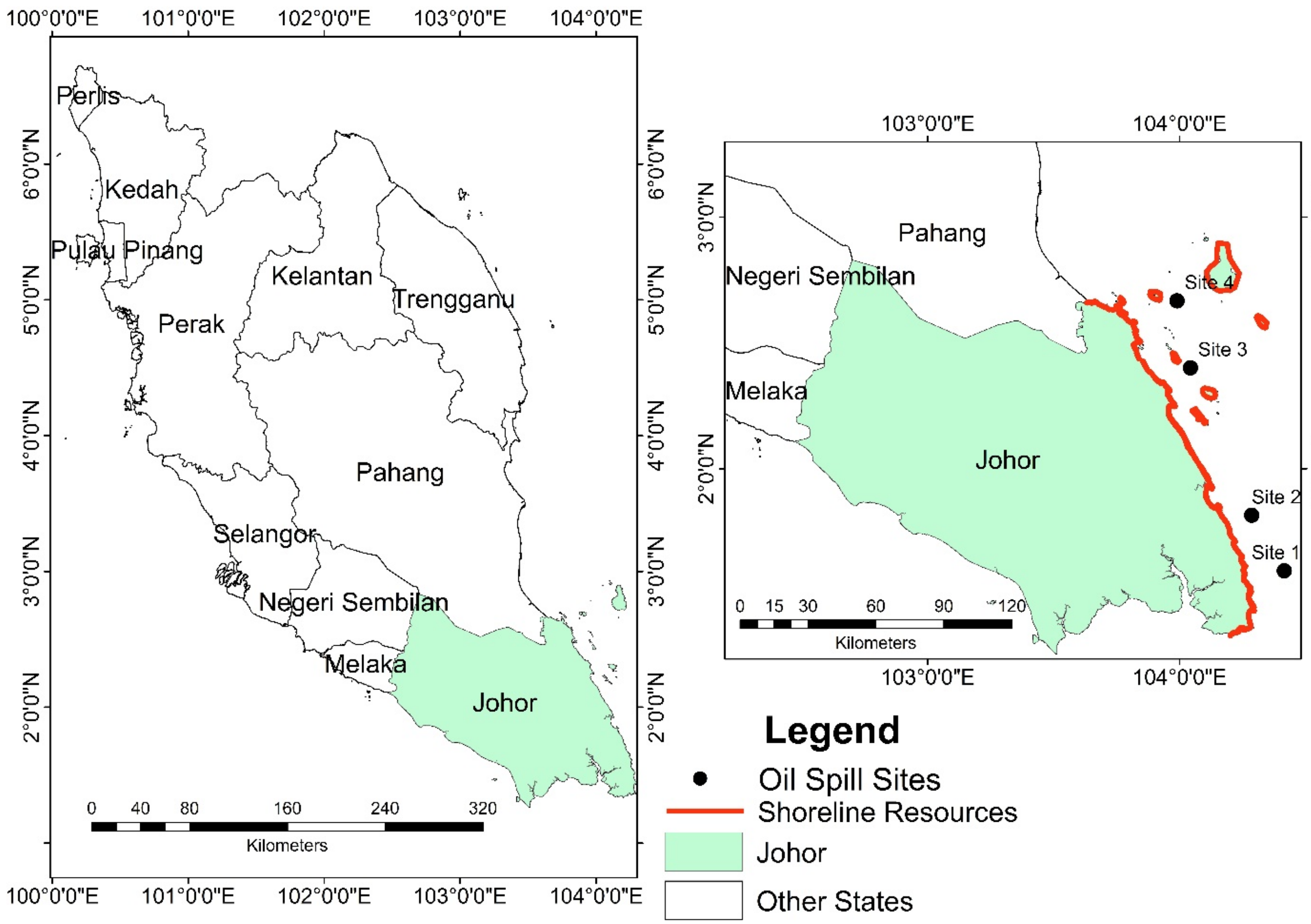

Figure 1. Map of Peninsular Malaysia showing the state of Johor and the study area's shoreline resources.

3.0 Materials and Method

3.1 Coastal Resources

The first step of this study was the development of a coastal resource map that comprises the physical shoreline types, biological and socio-economic features sensitive to oil spill. The classification of the map is based on the list from (IPIECA, 2012, Petersen et al., 2002), existing literature, satellite imagery observation and site visitation. The coastal resources map, which is a vector based map and an integral component of the oil spill decision support system (Kankara et al., 2016, Amir-Heidari and Raie, 2019, Sardi et al., 2020), was used to identify the elements of the coastal shorelines that are vulnerable to oil spill. This enables the emergency response team and decision-makers to holistically identify vulnerable zones in the occurrence of oil spills. Figure 2 shows the coastal resources map of the study area, highlighting the physical shoreline types which include building structures, muddy-shore, rocky-shore, sand/beach, and vegetation (marsh and mangrove). The biological elements include sub-tidal (mangrove and salt mash) and submerged plants (seagrass) while the socio-economic elements include the water way, recreational area, artificial lake and tourist zone (IPIECA, 2012, Petersen et al., 2002).

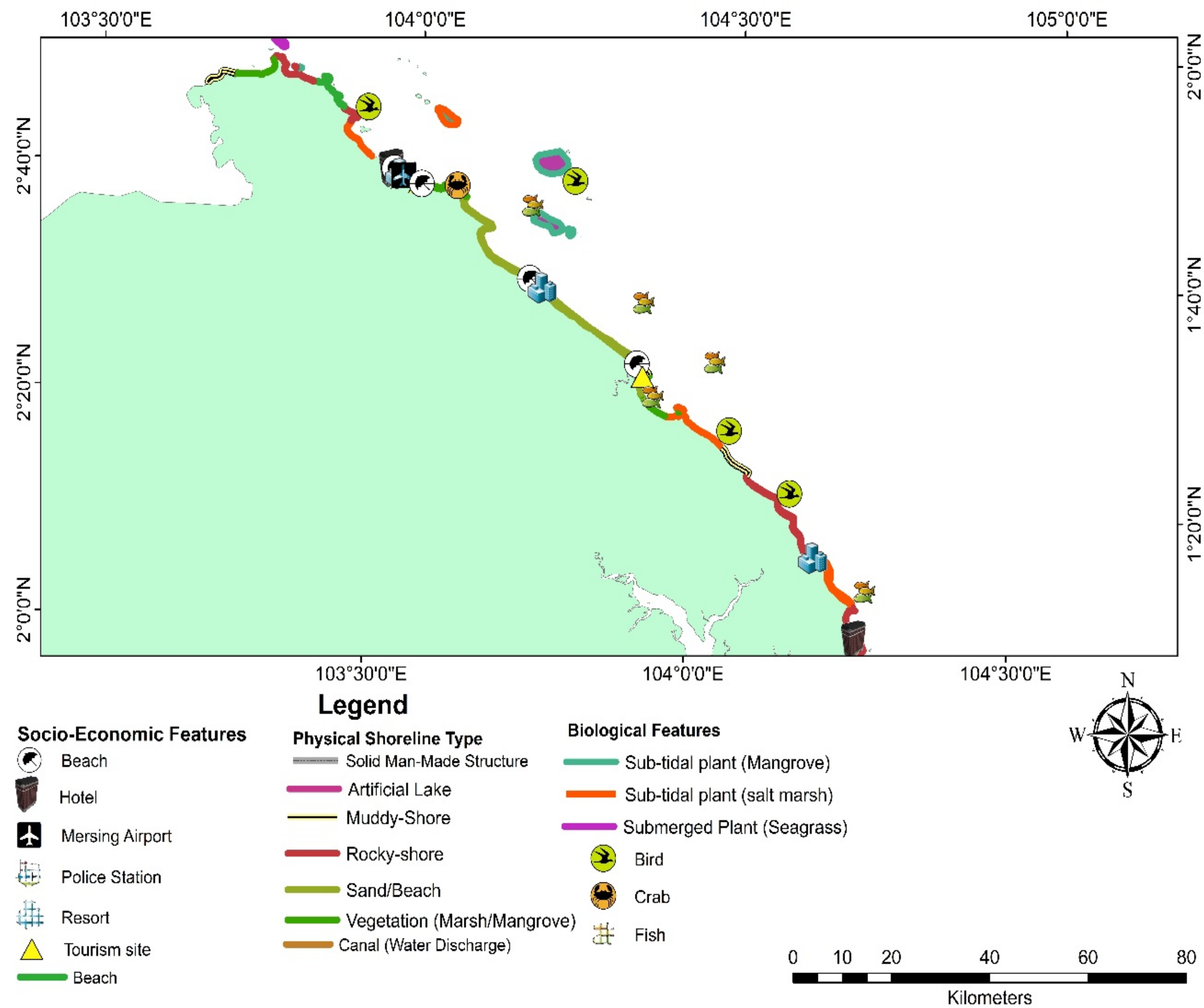

Figure 2. Map showing the coastal resources of the study area (Source: Authors)

3.2 Oceanographic Data

Reliable oceanographic data is an integral part of oil spill vulnerability mapping and the basis for accurate prediction. This is because it provides an overall view of the environmental factors that enable oil spill movement. Mean ocean currents, wind speed, wind direction, salinity, and ocean temperature for three different seasons (pre-monsoon, north-east monsoon and south-west monsoon) of the study area were used for this study (see Table 1). These data were sourced from GNOME online oceanographic data service (GOOD) that provides $1/12^0$ and 0.25^0 daily ocean current forecast data from Hybrid coordinate ocean model (HYCOM); and daily wind forecast data from the National Center for Environmental Prediction (NCEP) Global forecast system, respectively (Bleck, 2002). The acquired data was validated with data from existing literature and the Malaysian meteorology database to ensure accuracy and reliability of the outcome.

Table 1. Oceanographic parameters for oil spill vulnerability modelling.

Mean Oceanography Variable Period	**North East Monsoon (November-March)**	**Pre-Monsoon (April, October)**	**South West Monsoon (May-September)**
Wind speed (meter per hour)	4907.559^2	3488.90^2	4196.05^2
Wind direction	75^0	103^0	135^0
Salinity (parts per thousand (ppt))	32.5	32.5	32.5
Ocean temperature	29^0C	26^0C	28^0C
Ocean current speed (miles per hour)	761.15^2	992.43^2	833.80^2
Ocean current direction	220^0	25^0	40^0

3.3 Trajectory Modeling

The oil spill trajectory simulation was conducted using the GNOME model because of its high prediction accuracy (Xu et al., 2013, Chang et al., 2011, Farzingohar et al., 2011). The model is based on Langrangian discrete element which enables the simulation behavior of oil spill information of splots during the breaking process that includes spreading, evaporation, dispersion, and advection. The model is capable of simulating different oil spill types such as gasoline, diesel, medium oil, and kerosene at different volume and conditions such as continuous spill, instantaneous ship leak, intentional tank discharge, and leakage of tank. Thus, for this study, four oil spill sites were chosen to simulate oil spills during three different climatic conditions. A total of twelve different oil spill scenarios were simulated for 24 h using $100m^3$ medium (10,000 splots)

Malaysia BEKOK crude oil with 49.1 API (American Petroleum Institute) instantaneous ship tank discharge oil spill (See Supplementary File 1). The selection of this type of spill was based on the available data acquired from the Malaysia ministry of environment. The data shows that a larger percentage of oil spill in the study area is caused by ship discharge. Also, the mean oceanographic data (Table 1) were used as the predictive factors. The trajectory simulation produced different output which includes the time the slicks get to the coastal resources within the first 24 h; the speed of the slick, which is a function of the time the slick gets to the coastal resource and the distance of the oil spill point source to the coastal resources; slick trajectory direction; quantity of oil budget and the area of coastal resources affected at each scenario.

3.4 Vulnerability mapping

The vulnerability of the coastal resources to oil spill was ascertained using the shoreline resources properties layer (Figure 2) that comprises of socio-economic, biological and physical shoreline features of the coastal area and the GNOME trajectory output from the twelve oil spill scenarios during the three climatic seasons. The index of vulnerability was categorized into five classes: very-high (5), high (4), moderate (3), low (2) and very-low (1). The very low index represents areas with the least vulnerability to oil slick (splots) concentration. Low vulnerability depicts zones with low-density oil slick concentration and are far from the density point center. Moderate vulnerability zones contain significant oil slick concentration in a certain area while the high vulnerability areas comprise resources with significant oil slick (splots) and are near to the point center. Very high vulnerable zones comprise areas with high density of splots concentration which are also centered on a coastal resource (Sardi et al., 2020).

The first step in the production of the oil spill vulnerability map is the aggregation of the oil spill trajectory results from the four oil spill scenarios for the three different climatic seasons. The entire trajectory output of the Southwest monsoon from the four different scenarios were merged. A similar procedure was performed for the pre-monsoon and northwest monsoon in addition to aggregating all the twelve scenarios. The outputs were overlaid on the coastal resources (socio-economic, biological and physical feature) of the study area in the Geographical Information System (GIS) environment. The Kernel density spatial analysis function in ArcGIS was used to calculate the density of splots in the neighborhood around the coastal resources represented in the GIS layer. Thus, the vulnerability level/index of the coastal resources (Figure 2) were determined by overlaying the trajectory output and the coastal resources shapefile (Figure 3). From the output, an Environmental Vulnerability Index (EVI) table was developed for all the coastal elements in the study area.

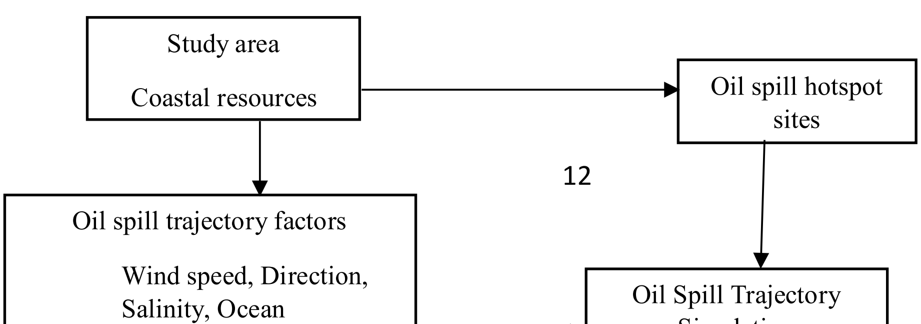

Figure 3. Modeling flowchart used in this study.

4.0 Results

4.1. Oil spill trajectory prediction

The results of the oil spill trajectory simulation are presented in Figure 4. Two different outcomes are indicated therein, which are the directional movement of the slick and the time the slick reaches the shoreline within the first 24 h of the spillage. It was observed from the outcome that the directions of the four experimental slick trajectories are similar, moving towards the southwest region of the area during the three climatic seasons. This is because the flow of water within the study area moves in the southwestern direction (Hoffman et al., 2015, Luu et al., 2015, Juneng and

Tangang, 2006, Chang et al., 2011), in addition to the ocean wave and current direction. It was also observed that the flow of water at the upper part (north) of the study area ('Pehang') moves towards the north while at the study area, the water moves towards the strait of Johor which is the southern part of Malaysia.

A variation in the time the slick reaches the shoreline was observed across the four different oil spill sites and seasons. The oil spill at site 1 had the slowest movement at 0.21 m/h, while the speed at site 2 was 0.62 m/h, site 3 was 0.96 m/h and site 4 was 0.83 m/h. Considering the climatic seasonality, variations were observed in the trajectory speed of the slick, with the least speed (0.62 m/h) recorded during the northeast monsoon. The speed in the southwest monsoon was 0.66 m/h and pre-monsoon had the highest speed at 0.68 m/h. These variations in speed are linked to the differences in the ocean current speed and wave speed which were also established by (Abascal et al., 2009, Guo and Wang, 2009), in addition to the location of the oil spill (See Table 2). In contrast to the study of Cheng et al. (2011) where only ocean current was identified as a major climatic factor influencing oil slick trajectory, both the ocean wave and current contribute significantly to the oil slick trajectory pattern in this present study. For example, Site 1 (Figure 4) is located in an almost enclosed sea area at the strait of Johor between Malaysia and Singapore, which allows lower forces to move the slick toward the shoreline unlike those at the open sea.

Also, the time taken for the slick to reach the shoreline varied across the three seasons, with the least time (16:00 h) recorded during the south-west monsoon and the longest time (24:00 h) during the north-east monsoon, indicating a lower effect on the shoreline. This can be attributed to the location of the oil spill site at an enclosed water path, causing the elements to move with the directional pattern of the water towards the open sea. In their study, Naidu et al. (2012) observed that the ocean current and wave at the open shore are stronger than that of close to shore. While the former produce a higher oil spill trajectory speed, the latter lowers the speed. The average time taken for the slick to reach the shoreline at the other sites is 7 h, with variations across the three climatic seasons. This is similar to the study of Deng et al. (2013) wherein variations in location and climatic parameters produced different oil travel distance and polluted area. The longest time taken by the slick to reach the shoreline was recorded in the northeast monsoon, aligning with our study's outcome. Please see (supplementary file 2) for the 24 h trajectory splots distribution outcome.

Table 2: Oil spill trajectory prediction

Site	Speed (m/h)	Climatic season	Speed (m/h)
Site 1	749.99	Northeast monsoon	2213.99
Site 2	2231.99	Pre-monsoon	2447.99
Site 3	3437.99	Southwest monsoon	2375.99
Site 4	2969.99		

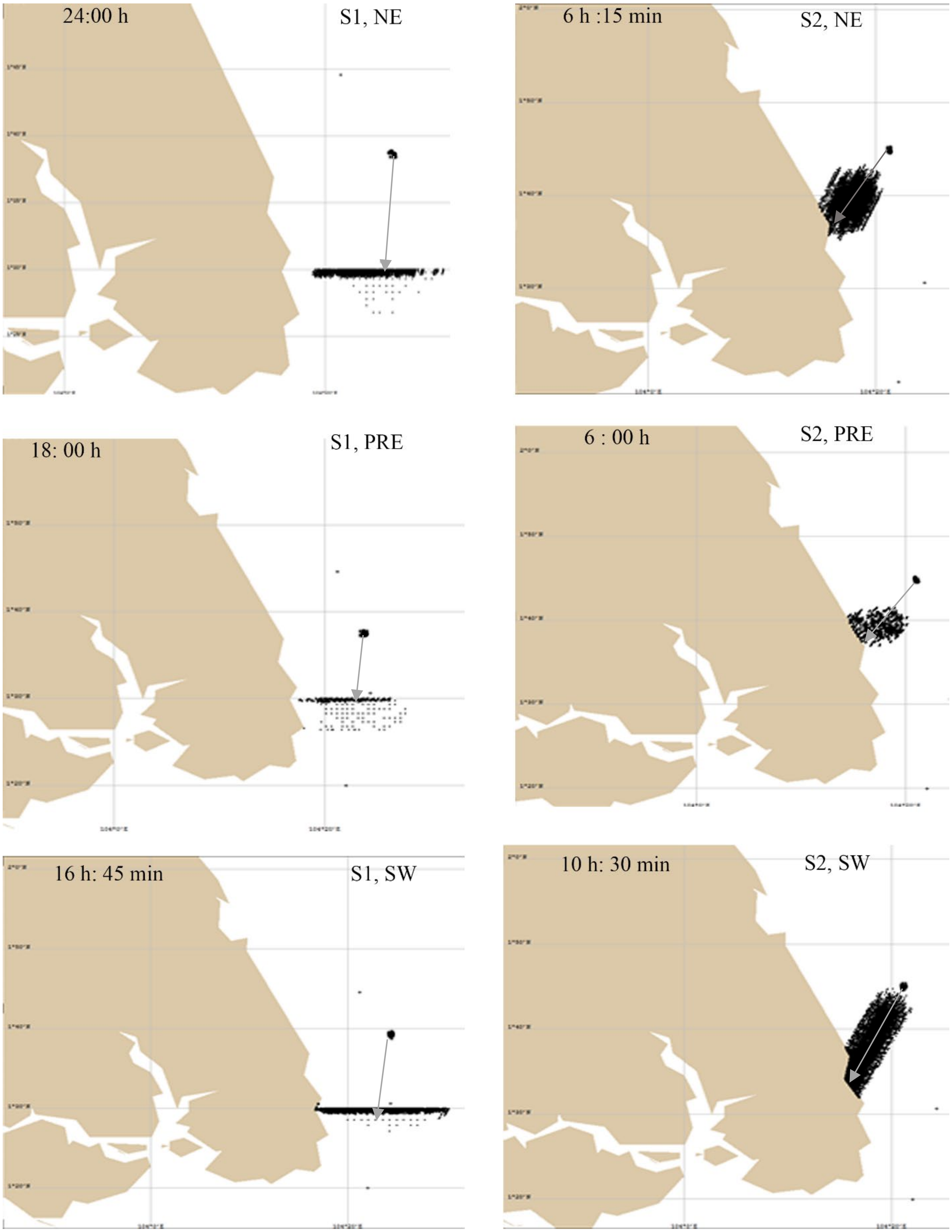
24:00 h
S1, NE
6 h :15 min
S2, NE
18: 00 h
S1, PRE
6 : 00 h
S2, PRE
16 h: 45 min
S1, SW
10 h: 30 min
S2, SW

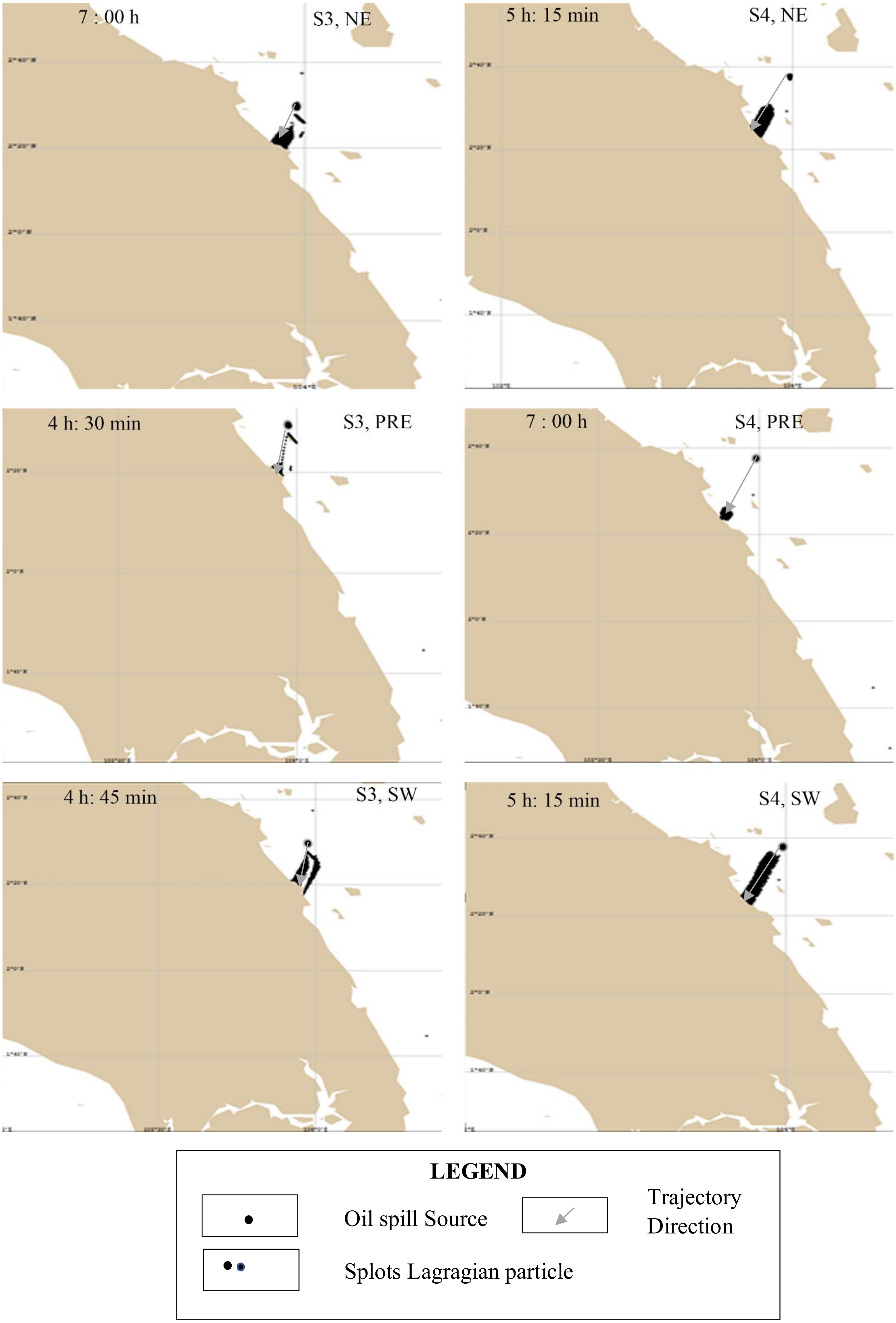
7 : 00 h
S3, NE
5 h: 15 min
S4, NE
4 h: 30 min
S3, PRE
7 : 00 h
S4, PRE
4 h: 45 min
S3, SW
5 h: 15 min
S4, SW
LEGEND
Oil spill Source
Trajectory Direction
Splots Lagragian particle

Figure 4. S1 (Site 1), S2 (Site 2), S3 (Site 3), S4 (Site 4), NW (northwest monsoon), SE (southeast monsoon), PRE (pre-monsoon) trajectory prediction output.

4.2 Estimation of oil spill budgeting and impact on coastal shoreline

4.2.1 Quantitative oil budget estimation

Understanding the different oil spill weathering processes such as evaporation, entrainment, emulsification, dissolution, biodegradation, photo-oxidation and sedimentation (Li et al., 2016, Spaulding, 2017) is important for measuring the extent of oil spill effects (Nelson et al., 2018, Qiao et al., 2019, Spaulding, 2017). Analysis of the oil spill quantitative budget estimation (Supplementary File 3) shows that evaporation, floating and spreading of the slick to the coastal line are the noticeable oil spill weathering processes that occurred during the spill in the study area. Qiao et al. (2019) identified 20% evaporation and 80% spreading over a period of 48 h at Tsushima strait, south and east coast of Japan. Also, Guo et al. (2009) observed advection, diffusion and mechanical spreading weathering at Dalian coastal region. From Figure 4, it was also observed that a higher proportion of the oil spill at site 1 was still floating on the water surface during the three seasons, in comparison to other sites. This implies that oil spilled within this location is highly unlikely to get to the shoreline, with a higher probability of remaining on the water body. In contrast, approximately 70% of the oil slick at the other sites get to the shoreline, impacting different elements while close to 27% evaporated and around 3% remain floating on the water column.

This outcome suggests that after the occurrence of an oil spill at the open sea/ocean, a higher percentage of the slick will reach the shoreline. For a similar occurrence at an enclosed sea area, much of the slick will remain on the water column within the first 24 h. This analysis offers valuable insights to emergency response teams to make appropriate decisions in combating oil spills at these locations. This confirms earlier findings that slick movement varies across locations and seasons. Liu et al. (2015) indicated that a higher percentage of spilled oil diffuse into the water column or sink beneath the sea at the Penglai 19-3 oil spill while Kankara et al. (2016) observed 40% of evaporation, 8% of dispersion along water column and 52% along the Chennai coastline of India.

4.2.2 Estimated Quantitative assessment of oil spill affected coastal resources

The estimated quantitative assessment of the coastal resources affected by oil spill was based on the output of the Kernel Density analysis which integrated results from the trajectory simulation at the four sites with the coastal resources information within the GIS environment. Table 3 illustrates the total area of coastal resources affected for each simulation. A total of 136.21 km^2 of shoreline coastal resources were affected with Vegetation (Marsh/Mangrove) being the most affected (55.42 km^2). Next to that was Rocky-shore with 36.35 km^2 affected area, sub-tidal plant (salt marsh), Sand/Beach, and Submerged Plant (Seagrass) representing 28.62 km^2, 10.23 km^2, and 5.59 km^2 affected areas respectively. The effects of the oil spill were higher during the Southwest monsoon with a total of 51.95 km^2 affected coastal resources while the least impact was identified during the northeast monsoon with approximately 34.91 km^2 of coastal resources being affected. Although all oil spill trajectory simulation scenarios were subjected to similar oil spill quantity (100m^3), oceanographic factors were varied. The highest oil spill impact on the shoreline was recorded at site 3, where approximately 46.85 km^2 of coastal resources were affected. This outcome indicates that physical shoreline natural resources are highly vulnerable to the impact of an oil slick, similar to the findings of (Kankara et al., 2016, Deng and Linda, 2018, Nelson et al., 2018, Sardi et al., 2020).

Table 3. Coastal resources affected by an oil spill

Spill scenario	**Artificial lake**	**Beach**	**Building structure**	**Canal (water discharge)**	**Muddy-shore**	**Rocky-shore (km^2)**	**Sand/beach (km^2)**	**Sub-tidal plant (mangrove)**	**Sub-tidal plant (salt marsh) (km^2)**	**Submerged plant (seagrass) (km^2)**	**Vegetation (marsh/mangrove) (km^2)**	**Total (km^2)**
S1NWMS	✓	✓	✓	✓	✓	✓	✓	✓	3.28	✓	✓	3.28
S1PREMS	✓	✓	✓	✓	✓	1.51	✓	✓	8.05	✓	✓	9.56
S1SWMS	✓	✓	✓	✓	✓	✓	✓	✓	0.87	✓	✓	0.87
S2NWMS	✓	✓	✓	✓	✓	13.68	✓	✓		✓	✓	13.68
S2PREMS	✓	✓	✓	✓	✓	10.64	✓	✓	3.9	✓	✓	14.54
S2SWMS	✓	✓	✓	✓	✓	10.52	✓	✓	3.39	✓	✓	13.91
S3NWMS	✓	✓	✓	✓	✓	✓	✓	✓		5.59	4.23	9.82
S3PREMS	✓	✓	✓	✓	✓	✓	4.22	✓	4.75	✓	7.33	16.3
S3SWMS	✓	✓	✓	✓	✓	✓	6.01	✓	4.38	✓	10.34	20.73
S4NWMS	✓	✓	✓	✓	✓	✓	✓	✓	✓	✓	8.13	8.13
S4PREMS	✓	✓	✓	✓	✓	✓	✓	✓	✓	✓	8.95	8.95
S4SWMS	✓	✓	✓	✓	✓	✓	✓	✓	✓	✓	16.44	16.44
Total	✓	✓	✓	✓	✓	36.35	10.23	✓	28.62	5.59	55.42	136.21

5.0 Discussion

5.1 Coastal oil spill Vulnerability mapping and Analysis

The oil spill vulnerability maps for this study were developed following the procedure in Section 3.4. The number of splots on each of the coastal resources after the trajectory simulation formed the basis of the vulnerability assessment of the resources. As depicted in Figures 5a-d, the vulnerability maps for the three climatic seasons and the aggregated map of all seasons show some level of similarities in the very-high and very-low vulnerability areas. However, differences exist in the vulnerability level of the coastal resources to the oil spill. There are also differences in the area extent of the different vulnerability indexes during the three seasons, which is linked to the variation in the climatic parameters used for the trajectory prediction. Amir-Heidari and Raie (2019) showed that change in parameters affect vulnerability. An example of such differences is seen in the area extent of each of the vulnerability classes (Figures 5a-d). During the Northeast monsoon, 36.56 km^2 of the area is very highly vulnerable to oil spill compared to 49.0 km^2, 40.1 km^2 and 35.21 km^2 of areas which are classified as very highly vulnerable areas during the southwest monsoon, pre-monsoon and the aggregation of the seasons, respectively. As presented in the supplementary file 4, across the three climatic seasons, vegetation (marsh/mangrove) is classified as the most very highly vulnerable among the different coastal resources with 36.56 km^2, 49.0 km^2, 37.66 km^2, and 35.21 km^2 affected areas in the northeast monsoon, pre-monsoon, southwest monsoon and the aggregated period, respectively. However, 2.44 km^2 of the rocky shore was equally indicated to be very highly vulnerable during the southwest monsoon.

Also, for the locations with high vulnerability, the area extent in the aggregated map (158.07 km^2) is higher than those in the northeast monsoon (102.76 km^2), pre-monsoon (97.9 km^2) and southwest monsoon (85.61 km^2) maps, respectively. A higher percentage of this high vulnerability zone is dominated by vegetation (marsh/mangrove) with 81.27 km^2 affected during the northeast monsoon, 86. 09 km^2 in pre-monsoon, 85.61 km^2 in the southwest monsoon, and 99.77 km^2 during the cumulative period. This is in addition to the 21.39 km^2 of rocky-shore in the northwest monsoon located in this high vulnerability zone. Also, 7.05 km^2 of beach , 34.31 km^2 of rocky-shore, and 16.94 km^2 of sub-tidal plant (salt marsh) are classified as highly vulnerable zones based on the cumulative period. Likewise, from Figures 5a and 5d on the one hand, and Figures 5b and c on the other hand, it is observed from the former that rocky shoreline elements and resort center have a high vulnerability which is contrary to the moderate vulnerability observed in Figures 5b and c where muddy shore, subtidal plant (mangrove), and tourist site were indicated to have low vulnerability to oil spill in this locality. This is due to the lower concentration of oil splots in the study area, similar to earlier studies (Kanniah et al., 2005, Najmuddin et al., 2019). Further analysis of the maps and the supplementary file 4 reveals that the physical elements at the shoreline (e.g. vegetable (marshy/mangrove)); biological elements (e.g. sub-tidal plant (salt marsh)) and socio-economic elements (e.g. Beach) are very highly and highly vulnerable to oil spill which could be linked to the directional movement of the oil slick. This is because the oil slick trajectory depends on the current oceanographic variables as indicated in section 3.2. Furthermore, aside from the vulnerability due to the elements' spatial dimensions, the economic cleaning cost and recovery period of the biological and physical shoreline resources are higher. For example, after the Deepwater Horizon oil spill, billions of US dollars were allocated for the cleaning of the different coastal resources (Grubesic et al., 2019, Taleghani and Tyagi, 2017). Similarly, shoreline resources like vegetation, salt marsh, and seagrass require more than eighteen months to recover after oil spill cleaning (Balogun et al., 2020). Also, the socio-economic resources are regarded as vital cultural and economic features of the study area (Kankara et al., 2016), which increases their vulnerability level.

Table 4 summarizes the outcome of this study's oil spill vulnerability analysis. Physical shoreline resources like Vegetation (Marsh/Mangrove) and biological features (Sub-tidal plant (salt marsh)) and other elements are prioritized in accordance to their vulnerability and overall impact in the coastal area while resources like man-made structures, police station and muddy shore have lower scores, which reflects their relative importance in terms of vulnerability to oil spill and overall impact in the coastal community as presented in the supplementary file 4.

For decision making, particularly when there is a conflict of interest regarding resources to be prioritized during emergency response to oil spills, physical shoreline and biological features should be given utmost attention because they require more cleaning and restoration resources for environmental sustainability compared to the equally sensitive socio-economic features.

Healthy vegetation sustains the ecosystem and is a source of revenue to the government (Tooke et al., 2010, Körner, 2009, Guay et al., 2014). They also act as carbon sinks to minimize Green House Gases (GHG) and reduce air pollution. Adamu et al. (2018), Ozigis et al. (2019a), Ozigis et al. (2019b), Balogun et al. (2020) highlighted that oil spills reduce the biomass and aboveground productivity of vegetation, which contributes to the reduction in environmental sustainability and food insecurity.

Table 4: Coastal resources oil spill environmental Vulnerability index.

Coastal resource types	Coastal shoreline features	Oil spill environmental vulnerability score
Socio-economic features	Beach	4
	Hotel	3
	Mersing airport	1
	Police station	1
	Resort	2
	Tourism site	1
	Canal (water discharge)	3
Physical shoreline	Solid man-made structure	1

	Artificial lake	2
	Muddy-Shore	1
	Rocky-Shore	5
	Sand/Beach	5
	Vegetation (marsh/mangrove)	5
Biological features	Sub-tidal plant (Mangrove)	3
	Sub-tidal plant (salt marsh)	5
	Sub merged plant (Seagrass)	3

Sub-tidal plants are also important and highly susceptible to oil spill, which will expose them to premature deaths and stunted growth. Thus, protecting them from environmental hazards such as oil spills should be prioritized. Silliman et al. (2012), McCall and Pennings (2012), Beazley et al. (2012), Turner et al. (2019) reported that over 30% sub-tidal plants were destroyed during the deep horizon oil spill. Such occurrences can be prevented in future by adopting EVI maps that provide reliable spatial vulnerability information to decision makers in order to facilitate prompt response with the potential to salvage the plants from destruction.

Beach, hotel, and resorts are major tourist facilities in Malaysia with approximately 12.3% contribution to the country's GDP and creating close to 1.5 million employment (Kadir and Karim, 2012). Risks to the beaches, hotels and resorts by oil spill will affect the tourism and services industry, with significant economic implications. This underscores the prioritization of these socio-economic features on the EVI map.

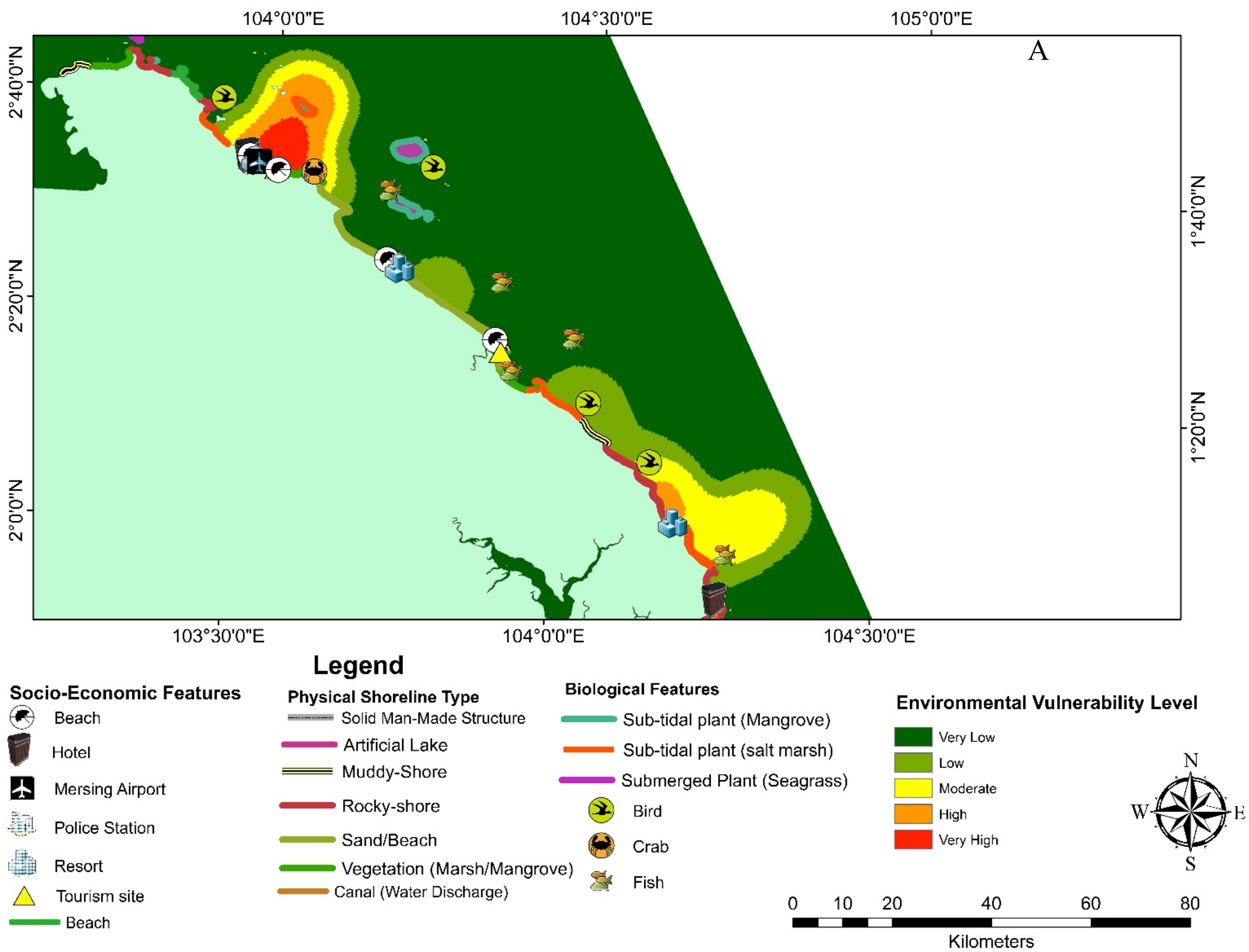
104°0'0"E
104°30'0"E
105°0'0"E
A
2°40'0"N
2°20'0"N
2°0'0"N
1°40'0"N
1°20'0"N
103°30'0"E
104°0'0"E
104°30'0"E
Legend
Socio-Economic Features
Beach
Hotel
Mersing Airport
Police Station
Resort
Tourism site
Beach
Physical Shoreline Type
Solid Man-Made Structure
Artificial Lake
Muddy-Shore
Rocky-shore
Sand/Beach
Vegetation (Marsh/Mangrove)
Canal (Water Discharge)
Biological Features
Sub-tidal plant (Mangrove)
Sub-tidal plant (salt marsh)
Submerged Plant (Seagrass)
Bird
Crab
Fish
Environmental Vulnerability Level
Very Low
Low
Moderate
High
Very High
N
W
E
S
0 10 20 40 60 80
Kilometers

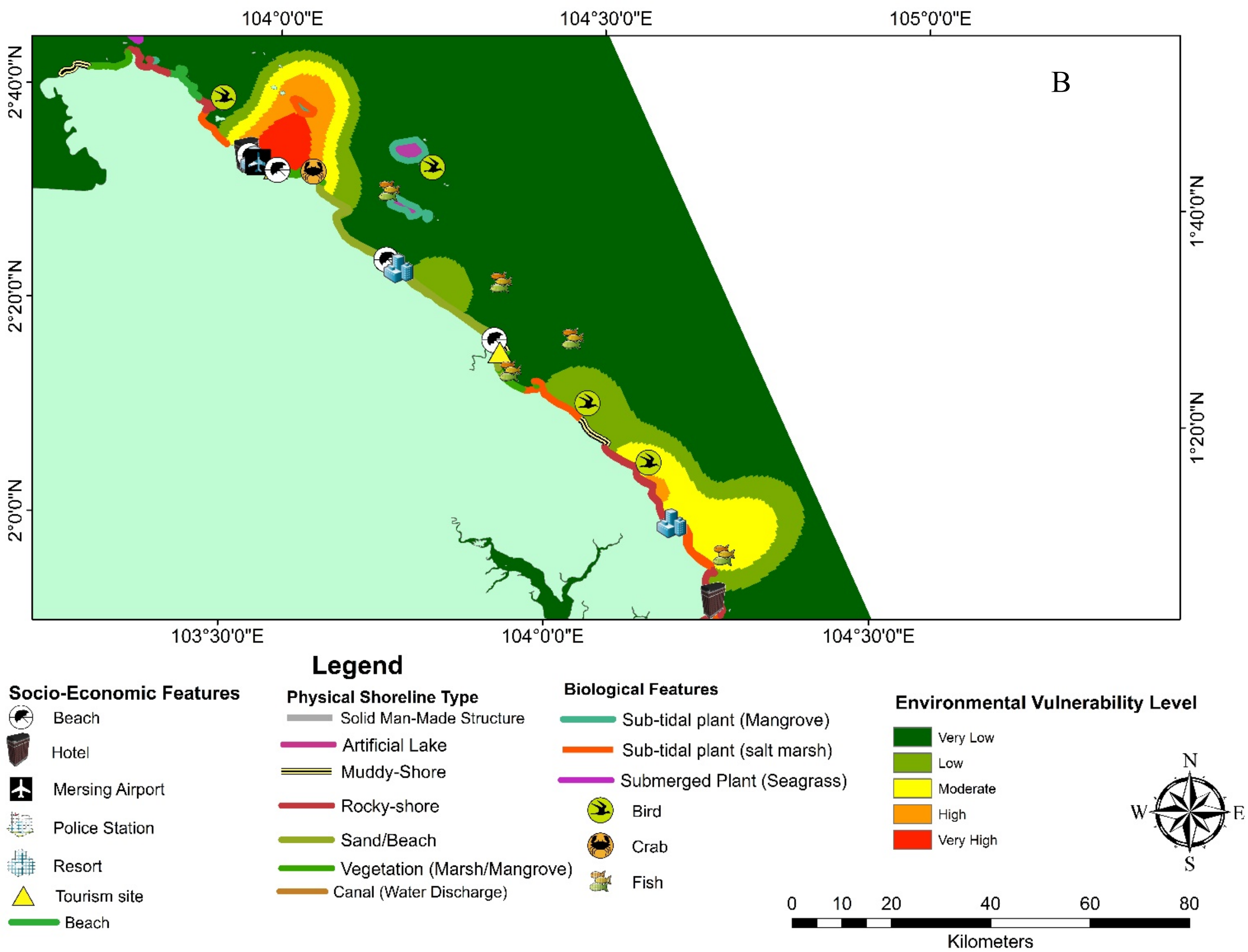
B
104°0'0"E
104°30'0"E
105°0'0"E
103°30'0"E
104°0'0"E
104°30'0"E
2°40'0"N
2°20'0"N
2°0'0"N
1°40'0"N
1°20'0"N
Legend
Socio-Economic Features
Beach
Hotel
Mersing Airport
Police Station
Resort
Tourism site
Beach
Physical Shoreline Type
Solid Man-Made Structure
Artificial Lake
Muddy-Shore
Rocky-shore
Sand/Beach
Vegetation (Marsh/Mangrove)
Canal (Water Discharge)
Biological Features
Sub-tidal plant (Mangrove)
Sub-tidal plant (salt marsh)
Submerged Plant (Seagrass)
Bird
Crab
Fish
Environmental Vulnerability Level
Very Low
Low
Moderate
High
Very High
N
W
E
S
0 10 20 40 60 80
Kilometers

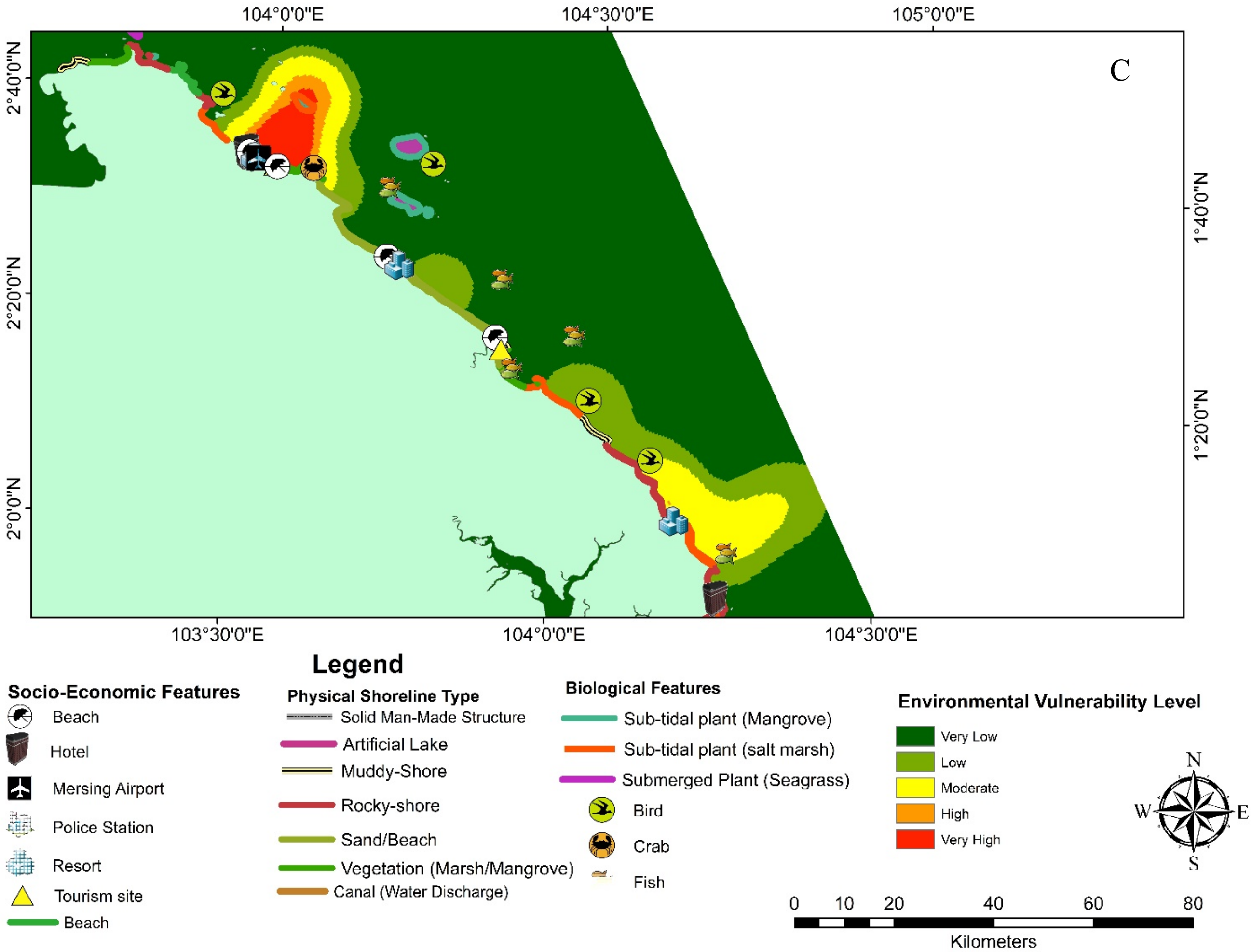
104°0'0"E
104°30'0"E
105°0'0"E
2°40'0"N
2°20'0"N
2°0'0"N
1°40'0"N
1°20'0"N
C
103°30'0"E
104°0'0"E
104°30'0"E
Legend
Socio-Economic Features
Beach
Hotel
Mersing Airport
Police Station
Resort
Tourism site
Beach
Physical Shoreline Type
Solid Man-Made Structure
Artificial Lake
Muddy-Shore
Rocky-shore
Sand/Beach
Vegetation (Marsh/Mangrove)
Canal (Water Discharge)
Biological Features
Sub-tidal plant (Mangrove)
Sub-tidal plant (salt marsh)
Submerged Plant (Seagrass)
Bird
Crab
Fish
Environmental Vulnerability Level
Very Low
Low
Moderate
High
Very High
N
W
E
S
0 10 20 40 60 80
Kilometers

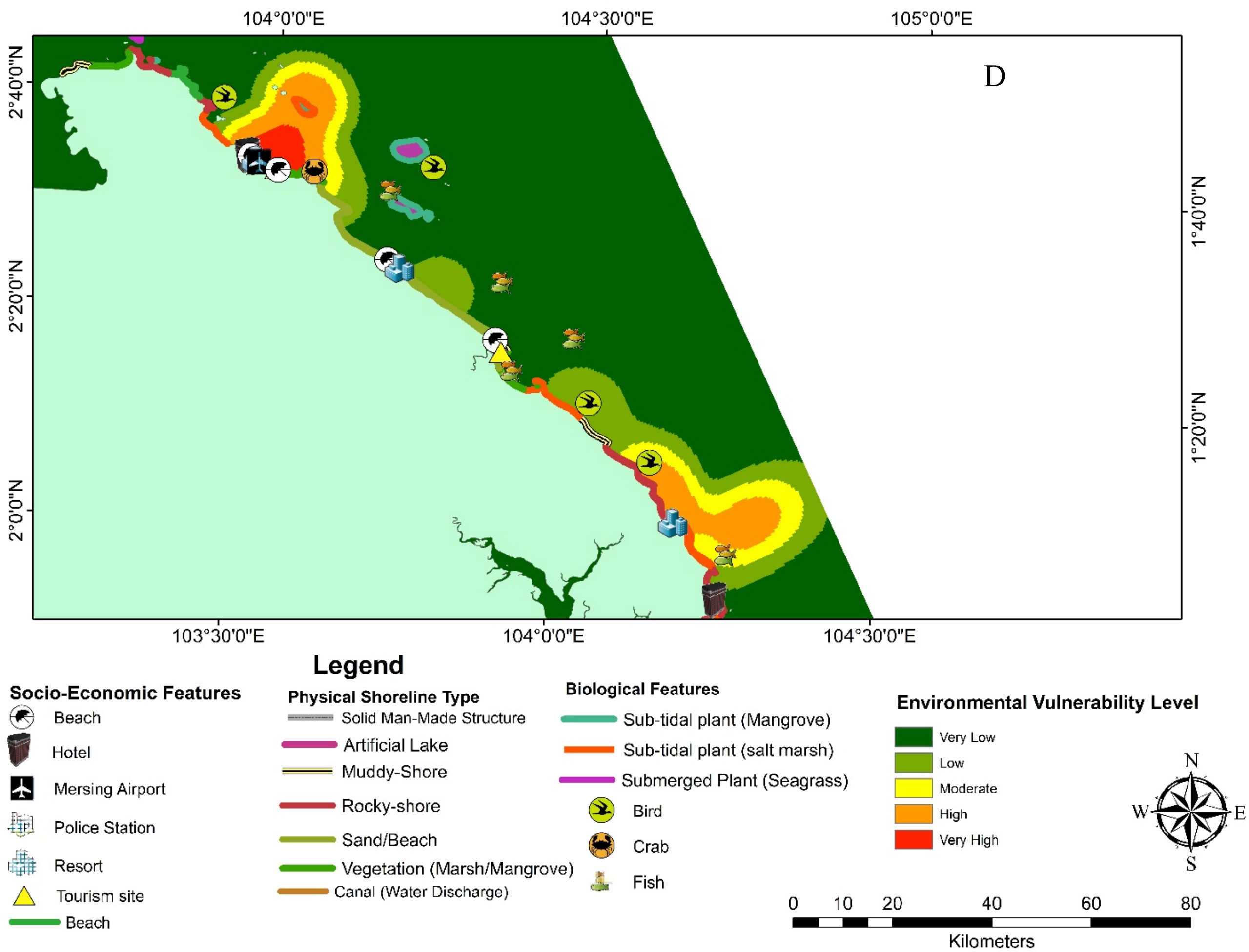

Figure 5: Coastal oil spill environmental vulnerability map: (a) northeast monsoon; (b) pre-monsoon; (c) southwest monsoon; and (d) cumulative/aggregated period.

5.0 Conclusion

Over time, coastal oil spill vulnerability maps have been based on expert opinion or trajectory models, without adequate consideration of seasonal climatic variations which influence the coastal sensitivity. This study has developed a coastal vulnerability map of Kota-Tinggi Johor, a hotspot of marine oil spill in South East Asia. The study takes into consideration the three climatic seasons, Northeast monsoon, Pre-monsoon and Southwest monsoon, oceanographic environmental factors, oil spill hotspot zones and the coastal resources in the study area (biological, physical shoreline and socio-economic resource). A 24 h simulation of medium crude oil spill trajectory from ship tank was conducted using GNOME model on four hotspot zones.

Findings of the study revealed that oil slick moves in a southwest direction, irrespective of the climatic season. This trend is linked to the Pacific Ocean flow direction. Significant differences were recorded in the flow speed of the slick over the three seasons, with the pre-monsoon period having the average highest speed at 0.68 m/h while the northeast monsoon has the least speed of 0.62 m/h. This indicates that emergency response mechanisms should be very active during the highly risky pre-monsoon season. Also, enclosed ocean paths experience slower oil slick flow than open ocean areas. Evaporation, floating and spreading are the major weathering processes that occurred during the oil spill trajectory analysis, with spreading being more dominant (70%), followed by evaporation (27%) and floating (3%) although the simulation seasons. This indicates that about 70% of oil slick will probably get to the coastal shoreline or similar proportion remain in water column in closed path water way 24 h after the occurrence of oil spill.

The quantitative impact assessment indicated that more of the shoreline resources are affected during the southwest monsoon, with vegetation (Marsh/Mangrove), rocky-Shore, beach, and sub-tidal plant (salt marsh) being the most susceptible elements while tourism site, solid man-made structures, and muddy-Shore are classified as the least vulnerability features within the study area. We conclude that variation in the climatic season significantly influence the level of coastal resources' sensitivity to oil spill. To enhance decision support for oil spill emergency response in the future, it is imperative to develop a web-based model to provide real time simulation and mapping of coastal resources' vulnerability to oil spill pollution thereby facilitating rapid response.

Abbreviation and terms:

The following abbreviations and terms were used in the manuscript:

h=hour(s)

m/h=meters per hour

m^3=meters cube

E=Eastern

N=Northern

EVI=Environmental Vulnerability Index

K^2=square kilometers

GDP=Gross Domestic Product.

Splots= this is the representative of oil spill in the GNOME spill trajectory model that appears as a pollutant particles in black.

Point source= This represent the oil spill source.

Acknowledgement

The authors gratefully acknowledge the financial support from the University Teknologi PETRONAS (UTP) Y-UTP Research Project Grant (015LC0-003). The National Ocean and Atmospheric Administration (NOAA)/Emergency Response Division (ERD) of the US Dept. of Commerce for making available the free GNOME software and oceanographic data available. Input from Mr Yusuf Aina, Dr. Mohammed Ozigis, Mr Caitlin O' Connor and Miss Lateefah Adeshewa are also acknowledged. The authors will equally like to appreciate the anonymous reviewers for their insightful comments and suggestions.

References

ABASCAL, A. J., CASTANEDO, S., MEDINA, R., LOSADA, I. J. & ALVAREZ-FANJUL, E. 2009. Application of HF radar currents to oil spill modelling. *Marine Pollution Bulletin,* 58**,** 238-248.

ABDUL-HADI, A., MANSOR, S., PRADHAN, B., TAN, C. J. E. M. & ASSESSMENT 2013. Seasonal variability of chlorophyll-a and oceanographic conditions in Sabah waters in relation to Asian monsoon—a remote sensing study. 185**,** 3977-3991.

ABDUL KARIM, S., ABD RAHMAN, Y. & ABDULLAH, M. J. 2004. Management of mangrove forests in Johor-as part of the coastal ecosystem management.

ADAMU, B., TANSEY, K. & OGUTU, B. 2018. Remote sensing for detection and monitoring of vegetation affected by oil spills. *International Journal of Remote Sensing,* 39**,** 3628-3645.

AKHIR, M., CHUEN, Y. J. J. J. O. S. S. & MANAGEMENT 2011. Seasonal variation of water characteristics during inter-monsoon along the east coast of Johor. 6**,** 206-214.

ALAA EL-DIN, G., AMER, A. A., MALSH, G. & HUSSEIN, M. 2018. Study on the use of banana peels for oil spill removal. *Alexandria Engineering Journal,* 57**,** 2061-2068.

AMIR-HEIDARI, P. & RAIE, M. 2019. A new stochastic oil spill risk assessment model for Persian Gulf: Development, application and evaluation. *Marine Pollution Bulletin,* 145**,** 357-369.

AZEVEDO, A., FORTUNATO, A. B., EPIFÂNIO, B., DEN BOER, S., OLIVEIRA, E. R., ALVES, F. L., DE JESUS, G., GOMES, J. L. & OLIVEIRA, A. 2017. An oil risk management system based on high-resolution hazard and vulnerability calculations. *Ocean & Coastal Management,* 136**,** 1-18.

BALOGUN, A.-L., MATORI, A.-N. & KIAK, K. 2018. Developing an Emergency Response Model for Offshore Oil Spill Disaster Management Using Spatial Decision Support System *J ISPRS Annals of Photogrammetry, Remote Sensing Spatial Information Sciences,* 4.

BALOGUN, A. L., YEKEEN, S. T., PRADHAN, B. & ALTHUWAYNEE, O. F. 2020. Spatio-Temporal Analysis of Oil Spill Impact and Recovery Pattern of Coastal Vegetation and Wetland Using Multispectral Satellite Landsat 8-OLI Imagery and Machine Learning Models. *Remote Sensing,* 12**,** 1225.

BEAZLEY, M. J., MARTINEZ, R. J., RAJAN, S., POWELL, J., PICENO, Y. M., TOM, L. M., ANDERSEN, G. L., HAZEN, T. C., VAN NOSTRAND, J. D. & ZHOU, J. J. P. O. 2012. Microbial community analysis of a coastal salt marsh affected by the Deepwater Horizon oil spill. 7**,** e41305.

BEYER, J., TRANNUM, H. C., BAKKE, T., HODSON, P. V. & COLLIER, T. K. 2016. Environmental effects of the Deepwater Horizon oil spill: a review. *Marine pollution bulletin,* 110, 28-51.

BISWAJEET, P., HAMID, A. J. R. J. O. C. & ENVIRONMENT 2009. Oil spill trajectory simulation and coastal sensitivity risk mapping. 13, 4.

BLACKBURN, M., MAZZACANO, C., FALLON, C. & BLACK, S. H. 2014. Oil in our oceans: a review of the impacts of oil spills on marine invertebrates. *The Xerces Society for Invertebrate Conservation, Portland, OR*.

BLECK, R. 2002. An oceanic general circulation model framed in hybrid isopycnic-Cartesian coordinates. *Ocean Modelling,* 4, 55-88.

BOZKURTOĞLU, Ş. N. E. 2017. Modeling oil spill trajectory in Bosphorus for contingency planning. *Marine Pollution Bulletin,* 123, 57-72.

CASTANEDO, S., JUANES, J. A., MEDINA, R., PUENTE, A., FERNANDEZ, F., OLABARRIETA, M. & POMBO, C. 2009. Oil spill vulnerability assessment integrating physical, biological and socio-economical aspects: application to the Cantabrian coast (Bay of Biscay, Spain). *J Environ Manage,* 91, 149-59.

CHANG, Y.-L., OEY, L., XU, F.-H., LU, H.-F. & FUJISAKI, A. 2011. 2010 oil spill: trajectory projections based on ensemble drifter analyses. *Ocean Dynamics,* 61, 829-839.

CHEN, J., ZHANG, W., WAN, Z., LI, S., HUANG, T. & FEI, Y. 2019. Oil spills from global tankers: Status review and future governance. *Journal of Cleaner Production,* 227, 20-32.

CHENG, Y., LI, X., XU, Q., GARCIA-PINEDA, O., ANDERSEN, O. B. & PICHEL, W. G. 2011. SAR observation and model tracking of an oil spill event in coastal waters. *Marine Pollution Bulletin,* 62, 350-363.

CHIU, C.-M., HUANG, C.-J., WU, L.-C., ZHANG, Y. J., CHUANG, L. Z.-H., FAN, Y. & YU, H.-C. 2018. Forecasting of oil-spill trajectories by using SCHISM and X-band radar. *Marine pollution bulletin,* 137, 566-581.

CLARK, R. B. 1992. Marine pollution.

DENG, Y. & LINDA, A. 2018. Assessing the Impact of Oil Spills on Marine Organisms. *Journal of Oceanography and Marine Research,* 6, 179.

DENG, Z., YU, T., SHI, S., JIN, J., JIANG, X., KANG, L., ZHANG, F. & WANG, W. 2013. Numerical Study of the Oil Spill Trajectory in Bohai Sea, China. *Marine Geodesy,* 36, 351-364.

DEPARTMENT FOR BUSINESS, E. I. S. 2019. GUIDANCE NOTES FOR PREPARING OIL POLLUTION EMERGENCY PLANS *In:* DEPARTMENT FOR BUSINESS, E. I. S. (ed.). Offshore Inspectorate, Department for Business, Energy and Industrial Strategy, AB1 Building, Crimon Place, Aberdeen, AB10 1BJ.

DEPELLEGRIN, D. & PEREIRA, P. 2016. Assessing oil spill sensitivity in unsheltered coastal environments: A case study for Lithuanian-Russian coasts, South-eastern Baltic Sea. *Mar Pollut Bull,* 102, 44-57.

FARZINGOHAR, M., IBRAHIM, Z. Z. & YASEMI, M. 2011. Oil spill modeling of diesel and gasoline with GNOME around Rajaee port of Bandar Abbas, Iran. *Iranian Journal of Fisheries Sciences,* 10, 35-46.

FERREIRA, A. M., MARQUES, J. C. & SEIXAS, S. 2017. Integrating marine ecosystem conservation and ecosystems services economic valuation: Implications for coastal zones governance. *Ecological Indicators,* 77, 114-122.

GŁUG, M. & WĄS, J. 2018. Modeling of oil spill spreading disasters using combination of Langrangian discrete particle algorithm with Cellular Automata approach. *J Ocean Engineering,* 156, 396-405.

GRUBESIC, T. H., NELSON, J. R. & WEI, R. 2019. A strategic planning approach for protecting environmentally sensitive coastlines from oil spills: Allocating response resources on a limited budget. *Marine Policy,* 108, 103549.

GUAY, K. C., BECK, P. S., BERNER, L. T., GOETZ, S. J., BACCINI, A. & BUERMANN, W. J. G. C. B. 2014. Vegetation productivity patterns at high northern latitudes: a multi-sensor satellite data assessment. 20**,** 3147-3158.

GUO, W., HAO, Y., ZHANG, L., XU, T., REN, X., CAO, F. & WANG, S. 2014. Development and application of an oil spill model with wave–current interactions in coastal areas. *Marine pollution bulletin,* 84**,** 213-224.

GUO, W. J. & WANG, Y. X. 2009. A numerical oil spill model based on a hybrid method. *Marine Pollution Bulletin,* 58**,** 726-734.

GUO, W. J., WANG, Y. X., XIE, M. X. & CUI, Y. J. 2009. Modeling oil spill trajectory in coastal waters based on fractional Brownian motion. *Marine Pollution Bulletin,* 58**,** 1339-1346.

GUO, W. J. E. P. 2017. Development of a statistical oil spill model for risk assessment. 230**,** 945-953.

HALPERN, B. S., FRAZIER, M., POTAPENKO, J., CASEY, K. S., KOENIG, K., LONGO, C., LOWNDES, J. S., ROCKWOOD, R. C., SELIG, E. R. & SELKOE, K. A. 2015. Spatial and temporal changes in cumulative human impacts on the world's ocean. *J Nature communications,* 6**,** 7615.

HAMILTON, J. D. & WU, J. C. 2014. Risk premia in crude oil futures prices. *Journal of International Money Finance* 42**,** 9-37.

HOFFMAN, J. M., PONNAMPALAM, L. S., ARAÚJO, C. C., WANG, J. Y., KUIT, S. H. & HUNG, S. K. J. T. J. O. T. A. S. O. A. 2015. Comparison of Indo-Pacific humpback dolphin (Sousa chinensis) whistles from two areas of western Peninsular Malaysia. 138**,** 2829-2835.

IPIECA, I. 2012. OGP (International Petroleum Industry Environmental Conservation Association, International Maritime Organization, International Association of Oil & Gas Producers) Sensitivity Mapping for Oil Spill Response. *Sensitivity mapping for oil spill response. London*.

JIANG, Z., HUANG, Y., CHEN, Q., ZENG, J. & XU, X. J. M. E. R. 2012. Acute toxicity of crude oil water accommodated fraction on marine copepods: the relative importance of acclimatization temperature and body size. 81**,** 12-17.

JUNENG, L. & TANGANG, F. T. J. J. P. S. 2006. The covariability between anomalous northeast monsoon rainfall in Malaysia and sea surface temperature in Indian-Pacific sector: a singular value decomposition analysis approach. 17**,** 101-115.

KADIR, N. & KARIM, M. Z. A. J. E. R.-E. I. 2012. Tourism and economic growth in Malaysia: Evidence from tourist arrivals from ASEAN-S countries. 25**,** 1089-1100.

KANKARA, R. S., AROCKIARAJ, S. & PRABHU, K. 2016. Environmental sensitivity mapping and risk assessment for oil spill along the Chennai Coast in India. *Mar Pollut Bull,* 106**,** 95-103.

KANNIAH, K. D., WAI, N. S., SHIN, A. L. M. & RASIB, A. W. Linear mixture modelling applied to IKONOS data for mangrove mapping. Ha Noi (VN): Asian Conference on Remote Sensing (ACRS2005), 2005. 7-16.

KILIAN, L. J. T. E. J. 2010. Explaining fluctuations in gasoline prices: a joint model of the global crude oil market and the US retail gasoline market. 31.

KÖRNER, C. 2009. *Mountain vegetation under environmental change*, na.

LEE, K., BOUFADEL, M., CHEN, B., FOGHT, J., HODSON, P., SWANSON, S. & VENOSA, A. J. O. T. R. S. O. C. 2015. The behaviour and environmental impacts of crude oil released into aqueous environments.

LI, P., CAI, Q., LIN, W., CHEN, B. & ZHANG, B. 2016. Offshore oil spill response practices and emerging challenges. *Marine Pollution Bulletin,* 110**,** 6-27.

LIU, X., GUO, J., GUO, M., HU, X., TANG, C., WANG, C. & XING, Q. 2015. Modelling of oil spill trajectory for 2011 Penglai 19-3 coastal drilling field, China. *Applied Mathematical Modelling,* 39**,** 5331-5340.

LUU, Q., TKALICH, P. & TAY, T. J. O. S. 2015. Sea level trend and variability around Peninsular Malaysia. 11.

MALAYSIA, D. O. S. 2013. *Johor at a Glance* [Online]. [Accessed 31 May 2019].

MCCALL, B. D. & PENNINGS, S. C. J. P. O. 2012. Disturbance and recovery of salt marsh arthropod communities following BP Deepwater Horizon oil spill. 7.

MELAKU CANU, D., SOLIDORO, C., BANDELJ, V., QUATTROCCHI, G., SORGENTE, R., OLITA, A., FAZIOLI, L. & CUCCO, A. 2015. Assessment of oil slick hazard and risk at vulnerable coastal sites. *Marine Pollution Bulletin,* 94**,** 84-95.

MENICAGLI, V., BALESTRI, E., VALLERINI, F., CASTELLI, A. & LARDICCI, C. 2019. Adverse effects of non-biodegradable and compostable plastic bags on the establishment of coastal dune vegetation: First experimental evidences. *Environmental Pollution,* 252**,** 188-195.

MIGNUCCI-GIANNONI, A. 1999. Assessment and rehabilitation of wildlife affected by an oil spill in Puerto Rico. *Environmental Pollution,* 104**,** 323-333.

NAGARAJAN, R., JONATHAN, M., ROY, P. D., WAI-HWA, L., PRASANNA, M. V., SARKAR, S. & NAVARRETE-LÓPEZ, M. J. M. P. B. 2013. Metal concentrations in sediments from tourist beaches of Miri City, Sarawak, Malaysia (Borneo Island). 73**,** 369-373.

NAIDU, V. S., SUKUMARAN, S., DUBBEWAR, O. & REDDY, G. S. 2012. Operational Forecast of Oil Spill Trajectory and Assessment of Impacts on Intertidal Macrobenthos in the Dahanu Region, West Coast of India. *Journal of Coastal Research,* 29**,** 398-409.

NAJMUDDIN, M., HARIS, H., SHAHROOL-ANUAR, R., NORAZLIMI, N., MD-ZAIN, B. & ABDUL-LATIFF, M. PrimaTourism: Plant selection by Schlegel's Banded Langur Presbytis neglectus in Johor. IOP Conference Series: Earth and Environmental Science, 2019. IOP Publishing, 012036.

NELSON, J. R., GRUBESIC, T. H., SIM, L. & ROSE, K. 2018. A geospatial evaluation of oil spill impact potential on coastal tourism in the Gulf of Mexico. *Computers, Environment and Urban Systems,* 68**,** 26-36.

NORDAM, T., BEEGLE-KRAUSE, C. J., SKANCKE, J., NEPSTAD, R. & REED, M. 2019. Improving oil spill trajectory modelling in the Arctic. *Marine Pollution Bulletin,* 140**,** 65-74.

OZIGIS, M. S., KADUK, J. D. & JARVIS, C. H. 2019a. Mapping terrestrial oil spill impact using machine learning random forest and Landsat 8 OLI imagery: a case site within the Niger Delta region of Nigeria. *Environmental Science and Pollution Research,* 26**,** 3621-3635.

OZIGIS, M. S., KADUK, J. D., JARVIS, C. H., DA CONCEIÇÃO BISPO, P. & BALZTER, H. 2019b. Detection of oil pollution impacts on vegetation using multifrequency SAR, multispectral images with fuzzy forest and random forest methods. *Environmental Pollution***,** 113360.

PETERSEN, J., MICHEL, J., ZENGEL, S., WHITE, M., LORD, C. & PLANK, C. J. N. T. M. N. O. 2002. Environmental sensitivity index guidelines. 192p., National Oceanic and Atmospheric Administration (NOAA). 11.

PIATT, J. F., LENSINK, C. J., BUTLER, W., KENDZIOREK, M. & NYSEWANDER, D. R. 1990. Immediate Impact of the 'Exxon Valdez' Oil Spill on Marine Birds. *The Auk,* 107**,** 387-397.

QIAO, F., WANG, G., YIN, L., ZENG, K., ZHANG, Y., ZHANG, M., XIAO, B., JIANG, S., CHEN, H. & CHEN, G. 2019. Modelling oil trajectories and potentially contaminated areas from the Sanchi oil spill. *Science of The Total Environment,* 685**,** 856-866.

ROCHA, F., HOMEM, V., CASTRO-JIMÉNEZ, J. & RATOLA, N. 2019. Marine vegetation analysis for the determination of volatile methylsiloxanes in coastal areas. *Science of The Total Environment,* 650**,** 2364-2373.

ROMERO, A. F., ABESSA, D. M. S., FONTES, R. F. C. & SILVA, G. H. 2013. Integrated assessment for establishing an oil environmental vulnerability map: Case study for the Santos Basin region, Brazil. *Marine Pollution Bulletin,* 74**,** 156-164.

SAKARI, M., ZAKARIA, M. P., MOHAMED, C. A. R., LAJIS, N. H., CHANDRU, K., BAHRY, P. S., MOKHTAR, M. B. & SHAHBAZI, A. 2010. Urban vs. Marine based oil pollution in the strait of Johor, Malaysia: a century record. *Soil Sediment Contamination* 19, 644-666.

SARDI, S. S., QURBAN, M. A., LI, W., KADINJAPPALLI, K. P., MANIKANDAN, P. K., HARIRI, M. M., TAWABINI, B. S., KHALIL, A. B. & EL-ASKARY, H. 2020. Assessment of areas environmentally sensitive to oil spills in the western Arabian Gulf, Saudi Arabia, for planning and undertaking an effective response. *Marine Pollution Bulletin,* 150, 110588.

SATPATHY, K. K., MOHANTY, A. K., NATESAN, U., PRASAD, M. V. R. & SARKAR, S. K. 2010. Seasonal variation in physicochemical properties of coastal waters of Kalpakkam, east coast of India with special emphasis on nutrients. *Environmental Monitoring and Assessment,* 164, 153-171.

SHEPPARD, C. R. 2000. *Seas at the millennium: an environmental evaluation: 1. Regional chapters: Europe, The Americas and West Africa*.

SILLIMAN, B. R., VAN DE KOPPEL, J., MCCOY, M. W., DILLER, J., KASOZI, G. N., EARL, K., ADAMS, P. N. & ZIMMERMAN, A. R. J. P. O. T. N. A. O. S. 2012. Degradation and resilience in Louisiana salt marshes after the BP–Deepwater Horizon oil spill. 109, 11234-11239.

SPAULDING, M. L. 2017. State of the art review and future directions in oil spill modeling. *Marine Pollution Bulletin,* 115, 7-19.

STATHAM, P. J. 2012. Nutrients in estuaries - An overview and the potential impacts of climate change. *Science of the Total Environment,* 434, 213-227.

TALEGHANI, N. D. & TYAGI, M. 2017. Impacts of Major Offshore Oil Spill Incidents on Petroleum Industry and Regional Economy. *Journal of Energy Resources Technology,* 139.

TAN, M. L., IBRAHIM, A. L., YUSOP, Z., DUAN, Z. & LING, L. 2015. Impacts of land-use and climate variability on hydrological components in the Johor River basin, Malaysia. *Hydrological Sciences Journal,* 60, 873-889.

TEMITOPE YEKEEN, S., BALOGUN, A. L. & WAN YUSOF, K. B. 2020. A novel deep learning instance segmentation model for automated marine oil spill detection. *ISPRS Journal of Photogrammetry and Remote Sensing,* 167, 190-200.

TOOKE, T. R., KLINKENBERG, B., COOPS, N. C. J. E., PLANNING, P. B. & DESIGN 2010. A geographical approach to identifying vegetation-related environmental equity in Canadian cities. 37, 1040-1056.

TRUSTEES, D. N. 2016. Deepwater Horizon oil spill: Final programmatic damage assessment and restoration plan and final programmatic Environmental Impact Statement. *Deepwater Horizon*.

TURNER, R. E., RABALAIS, N. N., OVERTON, E. B., MEYER, B. M., MCCLENACHAN, G., SWENSON, E. M., BESONEN, M., PARSONS, M. L. & ZINGRE, J. 2019. Oiling of the continental shelf and coastal marshes over eight years after the 2010 Deepwater Horizon oil spill. *Environmental Pollution,* 252, 1367-1376.

VAN WINDEN, J., SUIJKERBUIJK, B., JOEKAR-NIASAR, V., BRUSSEE, N., VAN DER LINDE, H., MARCELIS, A., COORN, A., PIETERSE, S., GANGA, K. & AL-QARSHUBI, I. The Critical Parameter for Low Salinity Flooding-The Relative Importance of Crude Oil, Brine and Rock. IOR 2013-17th European Symposium on Improved Oil Recovery, 2013. European Association of Geoscientists & Engineers, cp-342-00008.

XU, Q., LI, X., WEI, Y., TANG, Z., CHENG, Y. & PICHEL, W. G. 2013. Satellite observations and modeling of oil spill trajectories in the Bohai Sea. *Marine Pollution Bulletin,* 71, 107-116.

YANG, C., KAIPA, U., MATHER, Q. Z., WANG, X., NESTEROV, V., VENERO, A. F. & OMARY, M. A. 2011. Fluorous metal–organic frameworks with superior adsorption and hydrophobic properties toward oil spill cleanup and hydrocarbon storage. *Journal of the American Chemical Society,* 133, 18094-18097.

YEKEEN, S., BALOGUN, A. & AINA, Y. 2019. Early Warning Systems and Geospatial Tools: Managing Disasters for Urban Sustainability. *In:* LEAL FILHO, W., AZUL, A. M., BRANDLI, L., ÖZUYAR, P. G. & WALL, T. (eds.) *Sustainable Cities and Communities.* Cham: Springer International Publishing.
ZHANG, H. 2017. Transport of microplastics in coastal seas. *Estuarine, Coastal and Shelf Science,* 199**,** 74-86.